

Birefringent microstructures fabricated by two-photon polymerization containing an azopolymer

Vinicius Tribuzi,¹ Ruben Dario Fonseca,¹ Daniel Souza Correa,² and Cleber Renato Mendonça^{1,*}

¹Instituto de Física de São Carlos, Universidade de São Paulo, 13560-970, São Carlos, SP, Brazil

²Laboratório Nacional de Nanotecnologia para o Agronegócio (LNNA), Embrapa Instrumentação, 13560-970, São Carlos, SP, Brazil

*crmendon@ifsc.usp.br

Abstract: Birefringent materials have many applications in optical devices. An approach to obtain optically induced birefringence is to employ a guest-host strategy, using a polymer matrix containing an azodye. However, such method normally leads to low residual birefringence. Therefore, methodologies to produce microstructures with optimized birefringence are still on demand. Here we report on the fabrication, using two-photon polymerization, and characterization of birefringent microstructures produced in a polymer blend containing an azopolymer. Such microstructures present good structural integrity and residual birefringence of approximately 35 percent, depending on the sample formulation used, which indicates this approach for the fabrication of microoptical devices.

©2012 Optical Society of America

OCIS codes: (260.1440) Birefringence; (230.4000) Microstructure fabrication.

References and links

1. P. Rochon, J. Gosselin, A. Natansohn, and S. Xie, "Optically Induced and Erased Birefringence and Dichroism in Azoaromatic Polymers," *Appl. Phys. Lett.* **60**(1), 4–5 (1992).
2. C. R. Mendonça, U. M. Neves, L. De Boni, A. A. Andrade, D. S. dos Santos, Jr., F. J. Pavinatto, S. C. Zilio, L. Misoguti, and O. N. Oliveira, Jr., "Two-photon induced anisotropy in PMMA film doped with Disperse Red 13," *Opt. Commun.* **273**(2), 435–440 (2007).
3. S. P. Bian, J. A. He, L. Li, J. Kumar, and S. K. Tripathy, "Large photoinduced birefringence in azo dye/polyion films assembled by electrostatic sequential adsorption," *Adv. Mater.* **12**(16), 1202–1205 (2000).
4. Z. Sekkat, J. Wood, and W. Knoll, "Reorientation Mechanism of Azobenzenes within the Trans → Cis Photoisomerization," *J. Phys. Chem.* **99**(47), 17226–17234 (1995).
5. C. R. Mendonça, T. Baldacchini, P. Tayalia, and E. Mazur, "Reversible birefringence in microstructures fabricated by two-photon absorption polymerization," *J. Appl. Phys.* **102**(1), 013109 (2007).
6. J. F. Zu, J. Y. Guo, J. H. Si, G. D. Qian, M. Wang, and K. Hirao, "Effects of writing conditions on the photoinduced birefringence in azodye-doped polymers by a femtosecond laser," *Chem. Phys. Lett.* **421**(1-3), 101–105 (2006).
7. A. Dhanabalan, D. T. Balogh, C. R. Mendonça, A. Riul, C. J. L. Constantino, J. A. Giacometti, S. C. Zilio, and O. N. Oliveira, "Mixed Langmuir and Langmuir-Blodgett films of disperse red-13 dye-derivatized methacrylic homopolymer and cadmium stearate," *Langmuir* **14**(13), 3614–3619 (1998).
8. H. Xia, W. Y. Zhang, F. F. Wang, D. Wu, X. W. Liu, L. Chen, Q. D. Chen, Y. G. Ma, and H. B. Sun, "Three-dimensional micronanofabrication via two-photon-excited photoisomerization," *Appl. Phys. Lett.* **95**(8), 083118 (2009).
9. O. N. Oliveira, Jr., D. S. Dos Santos, Jr., D. T. Balogh, V. Zucolotto, and C. R. Mendonça, "Optical storage and surface-relief gratings in azobenzene-containing nanostructured films," *Adv. Colloid Interface Sci.* **116**(1-3), 179–192 (2005).
10. S. W. Magennis, F. S. Mackay, A. C. Jones, K. M. Tait, and P. J. Sadler, "Two-photon-induced photoisomerization of an azo dye," *Chem. Mater.* **17**(8), 2059–2062 (2005).
11. S. Maruo, O. Nakamura, and S. Kawata, "Three-dimensional microfabrication with two-photon-absorbed photopolymerization," *Opt. Lett.* **22**(2), 132–134 (1997).
12. S. Kawata, H. B. Sun, T. Tanaka, and K. Takada, "Finer features for functional microdevices," *Nature* **412**(6848), 697–698 (2001).

13. H. B. Sun, S. Matsuo, and H. Misawa, "Three-dimensional photonic crystal structures achieved with two-photon-absorption photopolymerization of resin," *Appl. Phys. Lett.* **74**(6), 786–788 (1999).
14. W. Haske, V. W. Chen, J. M. Hales, W. T. Dong, S. Barlow, S. R. Marder, and J. W. Perry, "65 nm feature sizes using visible wavelength 3-D multiphoton lithography," *Opt. Express* **15**(6), 3426–3436 (2007).
15. J. Fischer and M. Wegener, "Three-dimensional direct laser writing inspired by stimulated-emission-depletion microscopy," *Opt. Mater. Express* **1**(4), 614–624 (2011).
16. H. B. Sun, T. Tanaka, K. Takada, and S. Kawata, "Two-photon photopolymerization and diagnosis of three-dimensional microstructures containing fluorescent dyes," *Appl. Phys. Lett.* **79**(10), 1411–1413 (2001).
17. D. S. Correa, M. R. Cardoso, V. Tribuzi, L. Misoguti, and C. R. Mendonça, "Femtosecond Laser in Polymeric Materials: Microfabrication of Doped Structures and Micromachining," *IEEE J. Sel. Top. Quantum Electron.* **18**(1), 176–186 (2012).
18. D. S. Correa, V. Tribuzi, M. R. Cardoso, L. Misoguti, and C. R. Mendonça, "Selective excitation through tapered silica fibers of fluorescent two-photon polymerized structures," *Appl. Phys., A Mater. Sci. Process.* **102**(2), 435–439 (2011).
19. W.-S. Kuo, C.-H. Lien, K.-C. Cho, C.-Y. Chang, C.-Y. Lin, L. L. H. Huang, P. J. Campagnola, C. Y. Dong, and S.-J. Chen, "Multiphoton fabrication of freeform polymer microstructures with gold nanorods," *Opt. Express* **18**(26), 27550–27559 (2010).
20. K. Masui, S. Shoji, K. Asaba, T. C. Rodgers, F. Jin, X. M. Duan, and S. Kawata, "Laser fabrication of Au nanorod aggregates microstructures assisted by two-photon polymerization," *Opt. Express* **19**(23), 22786–22796 (2011).
21. T. Baldacchini, C. N. LaFratta, R. A. Farrer, M. C. Teich, B. E. A. Saleh, M. J. Naughton, and J. T. Fourkas, "Acrylic-based resin with favorable properties for three-dimensional two-photon polymerization," *J. Appl. Phys.* **95**(11), 6072–6076 (2004).
22. F. F. Dall'Agnol, O. N. Oliveira, and J. A. Giacometti, "Influence from the free volume on the photoinduced birefringence in azocompound-containing polymers," *Macromolecules* **39**(14), 4914–4919 (2006).

1. Introduction

Materials displaying photoinduced birefringence have been widely studied owing to their potential applications in optical devices such as optical data storage [1–3]. In the case of azocompounds, birefringence arises from a reversible photoisomerization (trans-cis-trans) and consequent molecular orientation [1,4]. While irradiated by linearly polarized light, the azochromophores undergo trans-cis-trans isomerization cycles, which are accompanied by molecular orientation. After several of these cycles, an excess of chromophores are aligned perpendicularly to the laser polarization, resulting in a macroscopic birefringence in the sample. When the excitation laser (writing beam) is turned off, some relaxation of the orientation occurs in the sample. Nevertheless, a considerable percentage of molecules remain oriented. Such optically induced birefringence can be observed by measuring the transmittance of a probe beam that passes through the sample when it is placed between two crossed polarizers. Aiming at applications in data storage devices, polymeric materials doped with azochromophores, presenting photoinduced birefringence, have been produced [4–8]. In such case, the guest-host strategy adopted to incorporate the azochromophore into the polymer led to low residual birefringence due to the high mobility of the chromophore in the polymeric matrix [9,10].

In this work, however, we report the fabrication of microstructures containing an azopolymer, which is expected to increase the residual birefringence. Thus, we prepared a polymeric blend containing the azocopolymer of 2-hydroxyethyl-methacrylate and 4-[*N*-ethyl-*N*-(2-methacryloxy-ethyl)]-amino-2'-chloro-4'-nitro-azobenzene (HEMA-DR13) and a tri-acrylic resin, used as the base resin for the microfabrication. The microstructures were obtained by two-photon polymerization (2PP), a technique that allows the fabrication of complex 3D topologies with no intrinsic constraints [11,12] and resolution below the diffraction limit [12–15]. Furthermore, by doping the resin used for 2PP with distinct compounds, some groups have achieved microstructures with interesting optical, biological and electrical properties [16–20]. The azopolymer-doped microstructures fabricated present birefringence when excited by an Ar⁺ laser operating at 514.5 nm. Because the azochromophore (DR13) is attached to the polymer backbone of HEMA-DR13 as a side chain, limiting the mobility of the azodye, we have been able to achieve a remaining birefringence of about 35% of the maximum birefringence value. These doped

microstructures open new possibilities for applications in micro optical devices such as micro optical storage and selective polarization devices.

2. Experimental

The experimental apparatus used for the fabrication of polymeric microstructures via two-photon polymerization (2PP) is composed by two movable mirrors, a precision motorized stage and a CCD camera for monitoring the fabrication. The laser source used is a Ti:Sapphire oscillator operating at 86 MHz and delivering 100-fs pulses centered at 790 nm. The pulsed laser beam is focused through a microscope objective (0.25 NA) into the resin, which is placed between two glass slides. In a region around the focal volume, light intensity is high enough to induce two-photon absorption and locally initiate the radical polymerization. Further details on this experimental setup can be found elsewhere [18]. After polymerization the sample is immersed in ethanol to wash away all uncured resin, leaving on the substrate only the fabricated microstructures.

The resin used for the microfabrication is composed by two three-acrylic monomers; tris(2-hydroxyethyl) isocyanurate triacrylate (resin A) and ethoxylated(6) trimethylolpropane triacrylate (resin B) [21]. Because guest-host systems, in which an azodye (such as DR 13) is dispersed in a polymeric matrix, usually present low residual birefringence (smaller than 10 percent), in this work we prepared a polymer blend of HEMA-DR13 and the acrylic resin (base resin). A solution of HEMA-DR13 in ethanol was mixed to the resin formulation, in a proportion of 0.75 weight % of the azopolymer, for approximately 1 hour. After mixing, the sample is left for 24 hours in a 50°C oven, for evaporation of the solvent. To this formulation we add the photoinitiator ethyl-2,4,6-trimethylbenzoyl phenylphosphinate [21] in 1.5 weight percent. The final formulation results in a red viscous liquid. A drop of this liquid is placed on a glass substrate between two spacers and then it is ready for the 2PP process. For comparison purposes we have also prepared macroscopic samples (thin films), which were polymerized using a UV-lamp, with the same composition of the 2PP microstructures.

To assess the induced birefringence, we measured the transmission of a linearly polarized He-Ne laser at 632.8 nm (reading beam) passing through the sample, that is located between two crossed polarizers. Birefringence is induced by exposing the sample to a linearly polarized Ar⁺ laser at 514.5 nm (writing beam).

3. Results and discussion

Typical structures are shown in the scanning electron microscopy (SEM) and bright field microscopy images presented in Figs. 1(a) and 1(b), respectively. For birefringence measurements on microscopic samples, we setup the apparatus illustrated in Fig. 2(a). To observe the light transmission through the sample, placed between crossed polarizer and analyzer we used a 0.25 NA microscope objective and a CCD camera. Figures 2(b) and 2(c) show, respectively, the image of the sample obtained with the reading beam (He-Ne laser) before turning the excitation laser on (Ar⁺ laser - writing beam) and after the writing beam exposure (one minute).

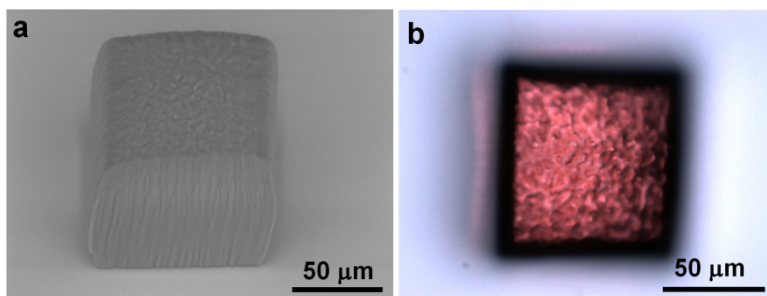


Fig. 1. Microscopy images of a microstructure containing HEMA-DR13. (a) Scanning electron micrograph and (b) bright field image.

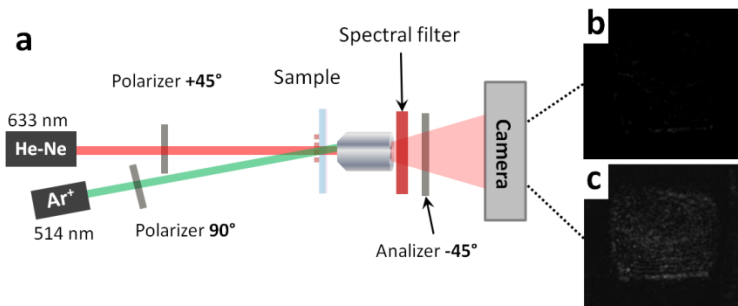


Fig. 2. (a) Experimental setup used to observe the optically induced birefringence in microscopic samples. (b) Image observed in the CCD camera before the writing beam irradiation and (c) after writing beam exposure (one minute).

Since the polarizer and analyzer are crossed, no light from the reading laser (He-Ne) is observed on the camera (Fig. 2(b)). A spectral filter is used to block any light coming from the writing laser. As the writing laser impinges the sample, reading laser transmission increases due to the photoinduced birefringence. Thus, reading beam light can pass through the analyzer (Fig. 2(c)), whereas other parts of the illuminated camera image area remain dark. Every sample passed through several writing and erasing cycles without any considerable damaging of their optical properties. To evaluate the influence of the resins on the residual optical memory, we have performed transmittance measurements in microscopic samples with different proportions of resin A and B. Sample 1 has 70% of resin A and 30% of resin B, while Sample 2 has 50% of each monomer. Both samples have the same amount of HEMA-DR13. Considering that resin A increases the rigidity of the resulting polymer [21], it is expected that samples with higher amount of this monomer will yield higher residual birefringence because relaxation of the aligned molecules will be decreased. For each sample we have performed transmittance measurements for different writing irradiances. Figure 3 shows the transmittance as a function of the exposure time for a macroscopic sample (thin film with the same composition of Sample 2), obtained with a writing beam irradiance of 140 mW/cm^2 .

In Fig. 3, no transmission of the reading beam is observed prior to the writing beam excitation, indicating the random orientation of the azochromophores. When the writing beam is turned on (point I), transmittance increases as a result of the induced birefringence in the material. When the writing beam is switched off (point II), the transmittance decreases to a saturation value (point III). The ratio between this value and the maximum signal is defined as the residual signal. As can be seen in Fig. 3, the residual signal we obtained for this sample is approximately 30 percent.

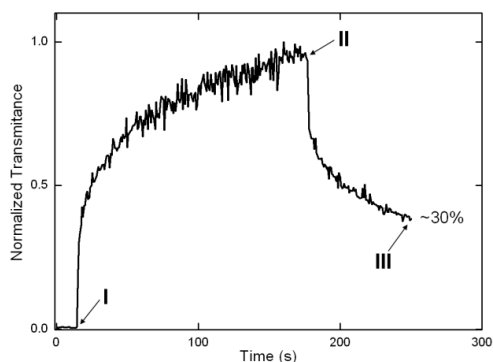


Fig. 3. Optically induced birefringence experiment for a macroscopic sample with Sample 2 composition (50 wt % of resin A and B). The writing beam irradiance for both samples is 140 mW/cm². The writing beam is turned on and off at points I and II, respectively. The point III denotes the residual signal after turning off the writing beam

Typical optically induced birefringence curves were also obtained for microstructures (as the one displayed in Fig. 1) with distinct compositions (Sample 1 and Sample 2). Figure 4 displays transmittance curves for a writing irradiance of 330 mW/cm². The optically induced birefringence (Δn) can be determined by measuring the probe beam transmittance after the analyzer, T , according to: $\Delta n = \lambda/\pi d \sin^{-1}\sqrt{T}$, where λ is the wavelength of the incident radiation and d is the sample thickness. By calibrating the transmission (T) from the image and considering the microstructure thickness ($\sim 100 \mu\text{m}$), we obtained $\Delta n = 4 \times 10^{-5}$.

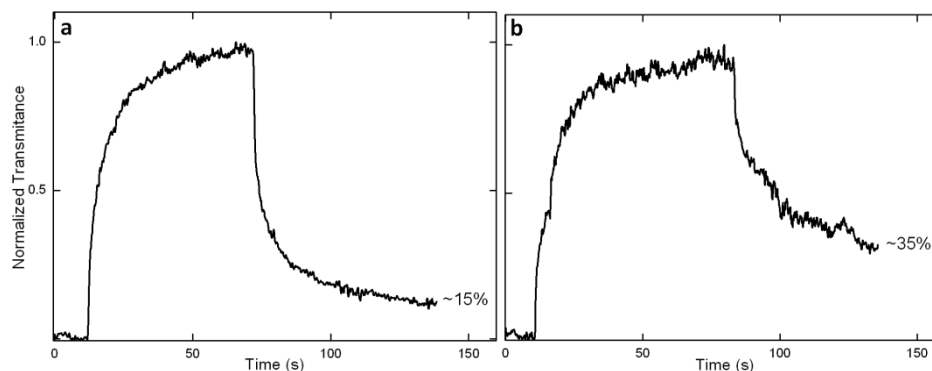


Fig. 4. Optically induced birefringence experiment for microstructures: (a) Sample 1 (70 wt % of monomer A and 30 wt % of B) and (b) Sample 2 (50 wt % of monomer A and B). The writing beam irradiance for both samples is 330 mW/cm².

While for Sample 1 we observe residual signals of about 15 percent, for Sample 2 these values are in the order of approximately 35 percent. Also, the maximum transmittance measured is higher for Sample 1, as indicated by the signal to noise ratio. These results show that, although Sample 1 has a higher relative amount of resin A, which increases the final structure rigidity, it actually presents a lower residual signal than Sample 2 (which has the same amount of the two resins). We believe that such behavior could be related to a larger free volume [22] in Sample 1. That extra space would allow a higher freedom of movement for the chromophores, making it easier either to align under illumination or to misalign when the writing laser is turned off. Decay times also depend on the free volume inside the polymer as does the residual transmittance signal.

The time evolution of the transmittance signal (rising curve, from point I to II) can be fitted with a bi-exponential function $T = A_f [1 - \exp(-t/\tau_f)] + A_s [1 - \exp(-t/\tau_s)]$, where the indices f and s refer, respectively, to fast and slow contributions to the optically induced

birefringence. The fast contribution is associated to the local mobility of the azo moieties, which is controlled by the interactions and free volume around them, while the slow contribution depends mainly on the mobility of the backbone polymer segments. By fitting transmittance signals (rising curves), similar to the ones in Figs. 4(a) and 4(b), at different writing beams intensities with the double-exponential function, we were able to obtain τ_f . Such results are summarized in Table 1.

Table 1. Fast Response Time as a Function of Writing Beam Intensities for Samples 1 and 2*

I(mW/cm ²)	Sample 1				Sample 2				
	A _f	τ _f (s)	A _s	τ _s (s)	A _f	τ _f (s)	A _s	τ _s (s)	
240 ± 10	0.92	3.5 ± 0.2	0.08	25	260 ± 20	0.90	4.3 ± 0.3	0.10	25
330 ± 20	0.98	2.3 ± 0.2	0.02	15	330 ± 20	0.97	3.5 ± 0.2	0.03	15
420 ± 30	0.99	1.9 ± 0.1	0.01	25	400 ± 30	0.99	2.2 ± 0.1	0.01	15

*The fitting errors for A_f, A_s and τ_s are, respectively ± 0.05, ± 0.02 and ± 5 s.

From the data in Table 1 we observe that the fast response component is the major contribution to the optically induced birefringence. Since the slow response time τ_s is associated with the motion of the polymer chain it is expected to be much slower (about 10 times) and basically independent of the experimental conditions, as we observed considering the fitting errors. As can be seen in Table 1, for all tested writing beam irradiances, Sample 1 presents smaller τ_f than Sample 2, indicating a higher free volume in Sample 1 in comparison to Sample 2, corroborating the smaller residual signal observed for Sample 1 (Fig. 4). This larger free volume is an effect of the lower total double bond conversion. During polymerization, the cross linking of the acrylic resin raises the glass transition temperature at a rapid rate, leading to a low mobility of free radicals. This in turn results in low conversion rates (reducing the amount of cross linking), leading to a higher free volume in the polymer. Therefore, although resin A provides greater hardness, it also reduces the total conversion rate rendering the sample higher free volume. This indicates that achieving high residual signal is not a simple matter of increasing polymer hardness. Our results show that an optimum point should be found in order to obtain maximum induced birefringence, which is a fundamental aspect for designing micro optical memory devices.

4. Conclusion

Using two-photon polymerization we fabricated microstructures from a blend composed by two acrylic resins and the azopolymer HEMA-DR13. The designed microstructures presented good residual birefringence and structural integrity. By using the azopolymer instead of a low molecular weight azodye, we could achieve high residual memories compared to previous results reported in the literature. By modifying the matrix polymer composition, we could optimize the residual induced birefringence of the microstructures. Through the analysis of the birefringence time-evolution curves we found that by decreasing the proportion of monomer A, responsible for providing hardness to the polymer microstructure, we could decrease the free volume in the material, giving less mobility to the azochromophores, which in turn increased residual optical memory. Our results show that increasing residual memory is not a matter of simply increasing polymer hardness, but depends on finding an optimum composition for the base resins and the azopolymer, which is a fundamental aspect for designing micro-optical storage devices.

Acknowledgments

The research described in this paper was supported by FAPESP, CNPq and CAPES from Brazil. Technical assistance from André L.S. Romero is gratefully acknowledged.